Published in final edited form as:
Cancer Res. 2008 November 15; 68(22): 9302–9310. doi:10.1158/0008-5472.CAN-08-2592.

PEA-15 Induces Autophagy in Human Ovarian Cancer Cells and is Associated with Prolonged Overall Survival

Chandra Bartholomeusz[1,2,6,*], **Daniel Rosen**[3,*], **Caimiao Wei**[4], **Anna Kazansky**[1,2,6], **Fumiyuki Yamasaki**[1,2], **Takeshi Takahashi**[1,2], **Hiroaki Itamochi**[1,2], **Seiji Kondo**[5], **Jinsong Liu**[3], and **Naoto T. Ueno**[1,2,6]

1*Breast Cancer Translational Research Laboratory, The University of Texas M. D. Anderson Cancer Center, Houston, TX 77030, USA*

2*Department of Stem Cell Transplantation and Cellular Therapy, The University of Texas M. D. Anderson Cancer Center, Houston, TX 77030, USA*

3*Department of Pathology, The University of Texas M. D. Anderson Cancer Center, Houston, TX 77030, USA*

4*Division of Quantitative Sciences, The University of Texas M. D. Anderson Cancer Center, Houston, TX 77030, USA*

5*Department of Neurosurgery, The University of Texas M. D. Anderson Cancer Center, Houston, TX 77030, USA*

6*Department of Breast Medical Oncology, The University of Texas M. D. Anderson Cancer Center, Houston, TX 77030, USA*

Abstract

Phospho-enriched protein in astrocytes (PEA-15) is a 15-kDa phosphoprotein that slows cell proliferation by binding to and sequestering extracellular signal-regulated kinase (ERK) in the cytoplasm, thereby inhibiting ERK-dependent transcription and proliferation. In previous studies of *E1A* human gene therapy for ovarian cancer, we discovered that PEA-15 induced the antitumor effect of *E1A* by sequestering activated ERK in the cytoplasm of cancer cells. Here, we investigated the role of PEA-15 in ovarian cancer tumorigenesis, the expression levels of PEA-15 in human ovarian cancer, and whether PEA-15 expression correlated with overall survival in women with ovarian cancer. We overexpressed PEA-15 in low-PEA-15-expressing cells and knocked down PEA-15 in high-PEA-15-expressing cells and analyzed the effect on proliferation, anchorage-independent growth, and cell cycle progression. We then assessed PEA-15 expression in an annotated tissue microarray of tumor samples from 395 women with primary epithelial ovarian cancer and tested whether PEA-15 expression was linked with overall survival. PEA-15 expression inhibited proliferation, and cell cycle analysis did not reveal apoptosis but did reveal autophagy, which was confirmed by an increase in LC3 cleavage. Inhibition of the ERK1/2 pathway decreased PEA-15-induced autophagy. These findings suggested that the antitumor activity of PEA-15 is mediated in part by the induction of autophagy involving activation of the ERK1/2 pathway. Multivariable analyses indicated that the women with high-PEA-15-expressing tumors survived longer than those with low-PEA-15-expressing tumors (hazard ratio = 1.973, $P = 0.0167$). Our findings indicate that PEA-15 expression is an important prognostic marker in ovarian cancer.

Correspondence: Naoto T. Ueno, Department of Breast Medical Oncology, Unit 1354, The University of Texas M. D. Anderson Cancer Center, 1515 Holcombe Boulevard, Houston, TX 77030. Phone: 713-794-4385; Fax: 713-794-4385; E-mail: E-mail: nueno@mdanderson.org.
*These authors contributed equally to this work.

Keywords

survival; autophagy; ovarian neoplasms; PEA-15; ERK

Introduction

Ovarian cancer is a major cause of cancer death among women in the United States. In 2007, 22,430 new cases are expected to be diagnosed and 15,280 women are expected to die of the disease; ovarian cancer will account for approximately 6% of all cancer deaths in women. Because very few ovarian cancers are detected at an early stage, understanding the molecular mechanisms of tumor development is crucial if more effective treatments are to be developed. Epithelial ovarian cancer is the most common type, accounting for 85% to 90% of all ovarian cancers. Currently, no definitive biomarkers have been identified for early detection of ovarian cancer; the only known biomarker in current use is CA125, a protein produced in increased amounts in 80% of ovarian cancer cases but also in benign conditions such as endometriosis, pregnancy, and liver disease (1).

In our previous study of gene therapy for ovarian cancer with the adenovirus type 5 gene *E1A*, we discovered that the antitumor effects of *E1A* resulted from the suppression of extracellular signal-regulated kinase (ERK) activity by phospho-enriched protein in astrocytes (PEA-15; also called PED), which sequestered phosphorylated ERK (pERK) in the cytoplasm (2). PEA-15 is an acidic, serine-phosphorylated, 15-kDa phosphoprotein that contains a death effector domain and is associated with microtubules. It blocks ERK-dependent proliferation by binding to ERK in the cytoplasm and preventing ERK entry into the nucleus. In NIH3T3 cells, this sequestration renders ERK unable to phosphorylate the transcription factor Elk-1, which is involved in ERK-dependent transcription (3). Genetic deletion of PEA-15 results in increased localization of ERK in the nucleus followed by increased cFos transcription and cell proliferation (3). Normal astrocytes containing high levels of PEA-15 can proliferate, but they do so more slowly than do PEA-15-depleted astrocytes (3). Thus, the expression level of PEA-15 seems to control the biological outcome of ERK/mitogen-activated protein kinase (MAPK) signaling by regulating the localization of ERK (3). However, we do not know how PEA-15 inhibits ovarian cancer cell growth or the clinical significance of PEA-15 expression levels in ovarian cancer.

In this study, we evaluated the role of PEA-15 in ovarian cancer cells *in vitro*. We found that PEA-15 resulted in inhibition of cell proliferation and induction of autophagy. Autophagy is a type of programmed cell death important in preventing cell aging and in providing the energy required for cell survival and repair during environmental stresses such as hypoxia, infection, and nutrient starvation (5,9). Two main pathways that regulate autophagy in response to starvation are the class I PI3K/Akt/mTor signaling pathway and the MAPK/ERK signaling pathway. The Akt/mTor pathway negatively regulates autophagy (4). Nutrient starvation, a known activator of autophagy, enhances ERK activity (5,6), and the ERK1/2 pathway is also stimulated in curcumin-induced autophagy (7). Conversely, MAPK/ERK activation is essential in lindane-induced carcinogenesis (8).

Further, we assessed the clinical significance of PEA-15 expression by comparing PEA-15 expression in a microarray of human ovarian cancer tissue specimens with clinical and pathological data on the specimen donors. Collectively, our findings indicate that PEA-15 expression may be an important prognostic marker in ovarian cancer.

Materials and Methods

Cell lines and culture conditions

OVCA-420, OVCA-432, and HEY ovarian cancer cells were kindly provided by Dr. Robert Bast of The University of Texas M. D. Anderson Cancer Center. OVCAR-3 ovarian cancer cells were obtained from the American Type Culture Collection (Manassas, VA) and PEA-15 expression was assessed in all four cell lines. OVCA-432 and HEY cells constitutively express high basal levels of PEA-15, whereas OVCAR-3 and OVCA-420 ovarian cancer constitutively express low basal levels of PEA-15. OVCA-420, OVCA-432, and HEY cells were grown in Dulbecco's modified Eagle's medium (DMEM)/F12 medium (GIBCO, Grand Island, NY); OVCAR-3 cells were grown in RPMI 1640 (GIBCO). In all cases, medium was supplemented with 2 mM L-glutamine, 10% fetal bovine serum, and penicillin/streptomycin, and cells were grown in a humidified incubator at 37°C with 5% CO_2.

Generation of Ad.PEA-15

We constructed an adenoviral PEA-15 vector (Ad.PEA-15) according to a protocol described previously (9). Briefly, hemagglutinin-tagged PEA-15 cDNA was subcloned into the adenovirus vector pAdTrack-CMV, in which the green fluorescence protein (GFP) is driven by the cytomegalovirus promoter and the PEA-15 cDNA is driven by a separate cytomegalovirus promoter. The control virus was an adenoviral vector expressing luciferase and green fluorescence protein (Ad.Luc). Infection efficiency was monitored in terms of the expression of green fluorescence protein (by fluorescence microscopy) and the expression of PEA-15 (by western blotting). We infected OVCAR-3 and OVCA-420 cells with either Ad.Luc or Ad.PEA-15, and 48 h later we observed the cells under a fluorescence microscope to test the efficiency of transfection (more than 80% of cells were green fluorescence protein positive (data not shown) and performed a western blot analysis to detect protein expression.

In vitro growth assays

For the *in vitro* growth experiments, OVCAR-3 cells (1×10^5 cells) or OVCA-420 cells (5×10^4 cells) were plated and exposed the next day to Ad.Luc or Ad.PEA-15 in serum-free medium for 1 h, followed by the addition of DMEM/F12 and incubation for 48 or 72 h. Cells were then harvested for western blotting (to assess protein expression) and trypan blue exclusion (to assess cell viability).

Western blot analysis

In preparation for western blotting, cells were washed three times with phosphate-buffered saline and then lysed in lysis buffer (20 mM Na_2PO_4 [pH 7.4], 150 mM NaCl, 1% Triton X-100, 1% aprotinin, 1 mM phenylmethysulfonyl fluoride, 100 mM NaF, and 2 mM Na_3VO_4) as described previously (10). PEA-15 was extracted with NP-40 lysis buffer (11). Primary antibodies were a rabbit anti-PEA-15 polyclonal antibody at 1:1,000 dilution (Synpep, Dublin, CA), anti-actin at 1:5,000 (Sigma-Aldrich Chemical Co, Saint Louis, MO), and polyclonal anti-LC3 antibody at 1:1000 (Covance, Denver, PA) (7). Secondary rabbit (1:5000) and mouse (1:5,000) fluorescent antibodies were from Molecular Probes (Eugene, OR) and were detected with an Odyssey imaging system (Li-Cor Biosciences, Lincoln, NE).

Fluorescence-activated cell sorting analysis

OVCAR-3 cells (1×10^5 cells) or OVCA-420 cells (5×10^4 cells) were plated and exposed the next day to Ad.Luc or Ad.PEA-15 in serum-free medium for 1 h, followed by the addition of DMEM/F12 and incubation for 24 h, 48 h, and 72 h. Apoptotic cells were analyzed by flow cytometry as described previously (10).

Quantification of acidic vesicular organelles by acridine orange staining

OVCAR-3 cells (1×10^5 cells) and OVCA-420 cells (5×10^4 cells) were plated and exposed the next day to Ad.Luc or Ad.PEA-15 in serum-free medium for 1 h, followed by the addition of DMEM/F12 and incubation for 72 h. To quantify the presence of acidic vesicular organelles (AVOs) indicative of autophagy, cells were stained with acridine orange (1 μg/ml) for 15 min. After trypsinization, cells were analyzed by using a FACScan flow cytometer and Cell Quest software (Becton Dickinson, San Jose, CA) (7).

Evaluation of anchorage-independent growth

To assess anchorage-independent growth, an indicator of *in vivo* tumorigenicity (12), we mixed cells with 0.5% agarose in complete medium at 37°C and poured the mixture over a layer of 1% agarose in complete medium in six-well plates. The top layer was allowed to solidify at 4° C for 20 min, and the plates were then incubated at 37°C for 3 weeks. At that point, cells were stained by the addition of *p*-iodonitrotetrazolium violet to each well and incubated at 37°C for 24 h, after which the colonies were photographed with a Zeiss microscope and counted by using the software provided with the microscope. Statistical analyses were done with GraphPad Prism software, version 4 (GraphPad Software, Inc., San Diego, CA). Data are presented as mean ± SE. Means for all data were compared by one-way ANOVA with post hoc testing.

siRNA transfection

OVCA-432 cells (2×10^5 per well) were seeded in six-well culture plates at 30% to 50% confluence. The next day, Oligofectamine (Invitrogen, Palo Alto, CA) was used to transfect cells with siPEA-15 (ggaagacaucccagcgaatt) or a scrambled siRNA duplex (siControl Non-Targeting siRNA #2) (Dharmacon Inc., Lafayette, CO) at a final siRNA concentration of 100 nM. After a 4-h incubation, FBS was added to a final concentration of 20% FBS in the wells, and cells were incubated for 48 h or 72 h, after which cells were harvested for western blotting (to determine protein expression) and trypan blue exclusion (to determine cell viability). Some cultures were treated with bromodeoxyuridine at 48 h and incubated for an additional 30 min (to assess DNA synthesis). Direct immunofluorescence staining was performed according to the manufacturer's protocol (Becton Dickinson), and the samples were analyzed on a Becton Dickinson FACScan flow cytometer.

OVCA-420 cells (5×10^4 per well) were seeded in six-well culture plates at 30% to 50% confluence. The next day, cells were transfected with Accell SMARTpool siERK or siH-Ras or Accell nontargeting siControl Pool (Dharmacon Inc., Lafayette, CO) at a final siRNA concentration of 1 μM. Forty-eight hours later, cells were infected with Ad.Luc or Ad.PEA-15 in serum-free medium for 1 h, followed by the addition of DMEM/F12 and incubation for 72 h. Then cells were harvested for western blotting (to determine protein expression) and stained with acridine orange (1 μg/ml) for 15 min. After trypsinization, cells were analyzed by using a FACScan flow cytometer and Cell Quest software.

Tissue microarrays

A tissue microarray was created from samples from 395 women with primary epithelial ovarian cancer who had undergone initial surgery at M. D. Anderson Cancer Center between 1990 and 2004. A separate microarray consisting of normal ovaries from 5 women without ovarian cancer, 5 with serous cysts, 5 with mucinous cysts, 10 with mucinous low-malignant-potential tumors, and 10 with serous low-malignant-potential tumors was used for comparison in the assessment of staining intensity. Tissue microarray blocks were constructed with a precision instrument (Beecher Instruments, Silver Spring, MD) as previously described (13,14).

The sample-tracking system for the ovarian cancer microarray was linked to a Microsoft Access database containing demographic, clinicopathologic, and survival data on the women who provided the samples. Variables available for analysis included histopathologic diagnosis (based on World Health Organization criteria), nuclear grade (based on Gynecologic Oncology Group criteria), and disease stage (according to the International Federation of Gynecology and Obstetrics system). Also considered in the analysis was extent of cytoreduction (optimal if residual disease after surgery was smaller than 1 cm or suboptimal if residual disease was larger than 1 cm). Time to events (death, relapse) was calculated from the date the tumor sample was obtained to the date of last contact or the event, whichever was earlier. Use of tissue blocks and chart review in the creation of the microarrays and the use of the microarrays for the studies described here were approved by the institutional review board of The University of Texas M. D. Anderson Cancer Center.

Immunohistochemical analysis

The tissue microarray slides were subjected to immunohistochemical staining as follows. After initial deparaffinization, endogenous peroxidase activity was blocked with 0.3% hydrogen peroxide. Deparaffinized sections were microwaved in 10 mM citrate buffer (pH 6.0) to unmask the epitopes. The slides were then incubated at 4°C overnight with antibody to PEA-15 (at 1:100 dilution; Synpep), followed by a 20-min incubation with biotin-labeled secondary antibody and then a 20-min incubation with a 1:40 solution of streptavidin:peroxidase. Tissues were then stained for 5 min with 0.05% 3′,3-diaminobenzidine tetrahydrochloride that had been freshly prepared in 0.05 M Tris buffer at pH 7.6 containing 0.024% hydrogen peroxide and then counterstained with hematoxylin, dehydrated, and mounted. All dilutions of antibody, biotin-labeled secondary antibody, and streptavidin:peroxidase were made in phosphate-buffered saline (pH 7.4) containing 1% bovine serum albumin. Negative controls were cultures in which the primary antibodies had been replaced with phosphate-buffered saline. All controls gave satisfactory results.

Immunostaining for PEA-15 and the proliferation marker Ki-67 was analyzed by computerized automated image analysis with an Ariol SL-50 system (Applied Imaging, San Jose, CA), in which mean relative optical densities were expressed as arbitrary units of intensity (15). Extent of staining was quantified with the whole core tissue at 20x magnification; the system is trained to consider only tumor epithelial cells in these measurements. Cytoplasmic immunostaining for PEA-15 was measured as the total integrated optical density and expressed in arbitrary optical density units. Cases displaying evidence of cytoplasmic PEA-15 staining were grouped by calculating the mean ± one SE of the total integrated optical density of all cases. Hence, cases were grouped as showing low, moderate, or high expression. For statistical analysis, all cases displaying total integrated optical density (mean ± SE) were then grouped together using a scale of 1 to 3 with cases exhibiting high or moderate expression (score 1 and 2) and low expression (score 3) (16). The Ki-67 labeling index was defined as the percentage of nuclear area showing positive staining for Ki-67; an index value of more than 15% was deemed high, and an index value of 15% or less was deemed low (17). Counting criteria and software settings were identical for all slides. Quantification was done by researchers unaware of the corresponding clinicopathologic information. Normal ovarian epithelial cells were used as a comparison for intensity and pattern of staining. The mean of the results from two core biopsy samples for each tumor specimen was calculated for each case.

Statistical analysis

The statistical analysis was based on all or a subset of the 343 patients whose tumor samples had been collected either at or just after first diagnosis of ovarian cancer and whose survival status was available. For overall survival, time to events was calculated from the date the tumor sample was obtained to the date of last contact or the date of death, whichever was earlier. In

the time-to-event analysis of overall survival, the number of observations included was slightly fewer than 343 because of missing data points for the covariates of interest.

Survival distributions were calculated with the Kaplan-Meier method to illustrate differences in overall survival by PEA-15 expression (low *vs.* moderate *vs.* high). The significance of apparent differences in time-to-events survival distribution between groups was tested with log-rank tests. *P* values of < 0.05 were considered statistically significant. Cox proportional hazards models were performed to assess whether there were associations between independent variables and overall survival. Each independent variable was first examined separately in a univariable Cox proportional hazards model with all possible data points. Graphic diagnostics for the linearity (specified functional form in the parametric part) of the Cox models were performed on the continuous variables by using martingale residual plots, with each factor being examined separately. Only independent variables that had *P* values of 0.10 or less in the univariable Cox model were examined in multivariable Cox models.

Results

PEA-15 overexpression inhibits ovarian cancer cell growth *in vitro*

We hypothesized that high PEA-15 expression inhibits cell proliferation in human ovarian cancer cells. We assessed PEA-15 expression in four human ovarian cancer cell lines OVCAR-3, OVCA-420, HEY, and OVCA-432. The OVCAR-3 and OVCA-420 cells expressed low amounts of PEA-15, and the HEY and OVCA-432 cells expressed high levels of PEA-15 (Fig. 1*A*). After confirming the equal transfection efficiency of Ad.Luc and Ad.PEA-15 in the OVCAR-3 and OVCA-420 cells (data not shown), we confirmed by western blotting that PEA-15 was expressed only in the Ad.PEA-15-infected cells and not in untreated or Ad.Luc-transfected cells (Fig. 1*B*). We also noted that pERK was induced after Ad.PEA-15 transfection (Fig. 1*C*).

To determine if PEA-15 overexpression could suppress cell growth, we infected OVCAR-3 and OVCA-420 ovarian cancer cells with Ad.Luc or Ad.PEA-15 and assessed cell viability by trypan blue exclusion 72 h later. Ad.PEA-15 suppressed the growth of OVCAR-3 cells by 28% and OVCA-420 cells by 25% compared with no suppression in Ad.Luc-infected cells (Fig. 1*D*) ($P < 0.05$). These results indicated that Ad.PEA-15 has a cytotoxic effect on ovarian cancer cells, resulting in growth inhibition. To determine whether the cytotoxicity of PEA-15 in OVCAR-3 and OVCA-420 cells was attributable to an increase in apoptosis, we used propidium iodide staining and flow cytometry. We treated OVCA-420 and OVCAR-3 cells with Ad.Luc and Ad.PEA-15 for 24 h, 48 h and 72 h. The sub-G1 fraction ranged from 0.6% to 5.22% in Ad.Luc-treated cells and from 0.54% to 4.47% in Ad.PEA-15-treated cells, indicating that Ad.PEA-15 did not increase apoptosis (supplemental Fig. S1).

Ad.PEA-15 induces autophagy in ovarian cancer cells

In light of its cytotoxicity in the absence of apoptosis, we next examined whether Ad.PEA-15 could induce autophagy. Indeed, we observed increased acidic vesicular organelles in OVCAR-3 and OVCA-420 cells that had been infected with Ad.PEA-15 (Fig. 2*A*). To further confirm autophagy, we examined the expression of LC3-I and its cleavage product LC3-II associated with the autophagosome membrane (18). In OVCA-420 cells, the ratio of LC3 II to LC3 I was larger in Ad.PEA-15-treated cells than in Ad.Luc-treated or untreated cells (Fig. 2*B*) indicative of autophagy. In OVCAR-3 cells, Ad.PEA-15 led to increases in both LC3 I and LC3 II compared with the levels in Ad.Luc-treated or untreated cells (Fig. 2*B*), findings that are characteristic of autophagy as seen in ceramide-induced autophagic cell death in malignant glioma cells (19). These results indicated that PEA-15 triggered both the conversion of LC3-I to LC3-II and the synthesis of LC3 protein.

As noted previously, we found that PEA-15 increased the expression level of pERK (Fig. 1*C*). Because ERK activation is known to result in autophagy during nutritional starvation (6), we next examined if abrogating ERK activation with the specific siRNA against ERK would reverse the autophagy. Indeed, treatment with siRNA against ERK suppressed both pERK expression (82%) and ERK expression (92%)(Fig. 2*C*) and reduced PEA-15-induced autophagy ($p<0.05$)(Fig. 2*D*). Since activation of ERK by PEA-15 expression has been shown to be a Ras-dependent mechanism (20), it was important to understand whether H-Ras signaling contributes to PEA-15-induced autophagy. However, we found that knock-down of H-Ras by siRNA (70%) resulted in enhanced PEA-15-induced autophagy (Fig. 2*D*).

PEA-15 knockdown increases proliferation of ovarian cancer cells

We then hypothesized that knockdown of PEA-15 expression in ovarian cancer cells increases their proliferation. Transfection of OVCA-432 cells with siRNA specific for PEA-15 reduced PEA-15 protein levels (Fig. 3*A*) and increased the number of cells by 115% compared with siControl ($P < 0.05$) (Fig. 3*B*). Next, we confirmed that siPEA-15 led to increased DNA synthesis, another hallmark of proliferation, relative to siControl (33.1% of cells proliferating *vs.* 17.47%; Fig. 3*C*). We also examined whether depletion of PEA-15 would facilitate the anchorage-independent growth of OVCA-432 cells, an indicator of *in vivo* tumorigenicity. The siPEA-15-treated OVCA-432 cells produced one and a half times as many colonies as did the siControl-treated cells ($P < 0.05$) (Fig. 3*D*), suggesting that silencing PEA-15 promoted cell growth through increasing DNA synthesis and anchorage-independent growth.

PEA-15 expression correlates with improved overall survival in women with ovarian cancer

At last we examined the clinical relevance of PEA-15 in ovarian cancer patients. Tissue microarray containing samples from 395 women with primary ovarian cancer were analyzed immunohistochemically. Tumors showed mostly cytoplasmic staining for PEA-15 (Fig. 4*A*), with some perinuclear and nuclear staining, consistent with our previous findings (2). Patient characteristics are summarized in Table 1. The median age was 60 years (range, 21–89). Most patients had stage III disease (68%), serous adenocarcinoma (77%), and tumors of nuclear grade 3 (91%). Most patients showed moderate expression of PEA-15 (69%) and low expression of PEA-15 (19%) and some patients showed high expression of PEA-15 (12%).

Univariable analysis showed that PEA-15 expression and well-known prognostic factors (e.g., patient age, histopathologic diagnosis, disease stage, nuclear grade, and extent of cytoreduction) were significantly associated with overall survival (Table 2). Univariable analyses did not reveal any significant associations between PEA-15 expression and any other variable, including histopathologic diagnosis, disease stage, nuclear grade, and extent of cytoreduction. Finally, we conducted multivariable analysis with a Cox proportional hazards model to assess the independent predictive value of PEA-15 expression along with other prognostic factors in ovarian cancer, we found that the women with high-PEA-15-expressing tumors survived longer than those with low-PEA-15-expressing tumors (hazard ratio = 1.973, $P = 0.0167$), and we found a marginal survival advantage for women with moderate-PEA-15-expressing tumors compared to those with high-PEA-15-expressing tumors (hazard ratio = 1.662, $P = 0.0527$). Kaplan-Meier overall survival curves by PEA-15 status are shown in Figure 4*B.* As expected, age, disease stage, and extent of cytoreduction also correlated with longer overall survival (Table 2).

Discussion

We showed here that PEA-15 expression in ovarian cancer cells inhibits their proliferation and induces autophagy. The preclinical finding was consistent with high levels of PEA-15 protein expression associated independently with improved overall survival in women with ovarian

cancer. The novelty of our findings is (1) the implication that the tumor-suppressive effects of PEA-15 in ovarian cancer result in part from PEA-15's induction of autophagy and (2) the demonstration that PEA-15 expression is an independent good prognostic factor.

Autophagy occurs in nutrient deprivation, in neurodegenerative diseases, in infectious diseases, and following treatment with chemotherapeutic agents (21). Autophagy has also been shown to be induced by the conditionally replicating adenovirus Ad.hTERT in malignant glioma cells (22). In agreement with our findings, other groups have shown that the MAPK pathway is an important regulator of autophagy. In particular, lindane-induced carcinogenesis is associated with sustained activity of ERK and disruption of autophagy (8); nutrient starvation enhances ERK activity and activates autophagy (23); curcumin induces autophagy and activates the ERK1/2 pathway (7); and ERK has been shown to phosphorylate Gα-interacting protein to induce autophagy in human colon cells (5). In light of these observations, we suggest that Ad.PEA-15 activates pERK and triggers autophagy in ovarian cancer cells. Further studies are needed to determine precisely how this takes place.

The major strengths of this study are our showing, for the first time, that a protein that binds ERK can induce autophagy that results in tumor-suppressive activity in ovarian cancer and that PEA-15 is related to improved overall survival in women with ovarian cancer. In addition, multivariable analyses indicated that the women whose tumors had moderate PEA-15 expression had marginally better survival compared to women whose tumors had high PEA-15 expression. One explanation for this could be that the number of patients with moderate PEA-15 expression was much higher than the number of patients with high PEA-15 expression. This analysis needs to be done again with a tissue microarray with large number of patient samples.

The effect of Ad.PEA-15 on induction of autophagy and induction of pERK differed by cell line, and PEA-15-induced autophagy was partially dependent on ERK in our experiments. The reason for this partial dependency may be involvement of other known pathways that regulate autophagy. These include the Akt/mTOR pathway, the death-associated protein kinase pathway, death-associated related protein kinase 1, BCL-2 and its family members, and the p38 pathway. We observed a slight suppression of mTOR expression; however there was no difference in the expression of the activated form, phospho-mTOR. We also observed a slight suppression of p-p38 expression. It was previously shown that p38 blockade in colorectal cancer cells induces autophagic cell death (24). Therefore, further studies are warranted to determine if the p38 pathway is involved in PEA-15-induced autophagy (supplemental Fig. S2).

In our experiments, Ad.PEA-15 induced autophagy in ovarian cancer cells was not dependent on H-Ras. The activation of ERK by PEA-15 expression has been shown as a Ras-dependent mechanism (20). However, Ras is also known to activate autophagy when it activates Raf and the ERK cascade and inhibit autophagy when it activates class I phosphatidylinositol-3 kinase (25). Indeed, Ras inhibitor augmented autophagy in oridonin-induced autophagy in HeLa cells (26). Other investigators have also shown that curcumin, the natural product B-group soyasaponins, and the lipid-soluble cardiac glycoside activate ERK1/2, inducing autophagy (7,27,28). It has been suggested that the signal strength, duration, and substrate expression may result in ERK activity resulting in one physiological outcome *vs.* another (e.g., cell proliferation, autophagy). Recently, it was shown that PEA-15 may act as a scaffold for ERK and RSK2 molecules, resulting in increasing ERK activation of RSK2 leading to a specific physiological outcome (29). Thus, further study is needed before one can generalize the results whether PEA-15 induced autophagy is not dependent on Ras.

Whether PEA-15 has similar functions in other types of cancer is unknown. In a previous study of a tissue microarray consisting of samples from patients with breast cancer, the loss of

PEA-15 expression correlated with increased invasiveness, but no survival data were shown (30). We are currently attempting to confirm our findings regarding ovarian cancer in a large tissue microarray consisting of samples from patients with breast cancer and assess possible correlations of PEA-15 expression with tumor stage and overall survival in breast cancer.

Another possible mechanism to explain the antitumor effect of PEA-15 is its ability to inhibit invasion by binding to ERK1/2 and preventing the phosphorylation of its nuclear substrate (30). The phosphorylation status of PEA-15 also affects its ultimate effects; phosphorylated protein can lead to increased proliferation and inhibited apoptosis, whereas unphosphorylated PEA-15 binds ERK1/2, blocking its nuclear translocation and cellular proliferation (31,32). We have yet to determine the phosphorylation status of PEA-15 in the samples in our tumor tissue microarray. It is also possible that the site at which PEA-15 is phosphorylated is a factor in its activity, another issue being addressed in our laboratory. Our findings from the current study provide a foundation that allows us to take the next steps in determining whether PEA-15 is a novel biomarker that can predict clinical outcomes in patients and in the development of PEA-15-targeted therapy for ovarian cancer.

Our findings are consistent with those of other groups that have found that PEA-15 inhibits cell proliferation (3), inhibits astrocyte motility through a pathway that depends on the delta isoform of protein kinase C (33), and may have a tumor suppressive function by controlling the localization of pERK (34). Our own previous work showed that PEA-15 by itself was able to suppress colony formation in breast and ovarian cancer cell lines and that part of the antitumor effect of *E1A* in ovarian cancer resulted from the cytoplasmic sequestration of the activated form of ERK by PEA-15 (2.). In contrast to our findings, others have shown that PEA-15 inhibits apoptosis induced by the fas ligand, tumor necrosis factor-α, and tumor necrosis factor-related apoptosis-inducing ligand (11,35,36). Trencia et al reported that Akt phosphorylates PEA-15, thereby stabilizing its antiapoptotic function (37). PEA-15 has also been shown to promote skin tumors (38) and is overexpressed in transformed and metastatic murine squamous carcinoma cells (39), suggesting that PEA-15 has both antiapoptotic and tumorigenic functions. Some of the differences between our study and others could be due to the phosphorylation status of PEA-15, which may be important in determining whether PEA-15 regulates cell proliferation or apoptosis (31,32). Further studies regarding the phosphorylation of PEA-15 are needed to clarify the role of PEA-15 in cancer.

In conclusion, we have shown for the first time that the antitumor activity of PEA-15 is due in part to induction of autophagy and that high PEA-15 expression is associated with improved overall survival in women with ovarian cancer.

Supplementary Material

Refer to Web version on PubMed Central for supplementary material.

Acknowledgments

We thank Christine Wogan and Stephanie Deming of the Department of Scientific Publications at M. D. Anderson Cancer Center for their expert editorial assistance and Wendy Schober of the Flow Cytometry and Cellular Imaging Core Facility at M. D. Anderson Cancer Center.

Grant support: National Institutes of Health (NIH) grant CA127562 and Sprint for Life Fund for Blanton-Davis Ovarian Cancer Research Program (N.T. Ueno), Nellie B. Connally Breast Cancer Research Fund (Breast Cancer Translational Research Laboratory), NIH grant CA016672-29 (Flow Cytometry and Cellular Imaging Core Facility at M. D. Anderson Cancer Center), and a Betty Anne-Murray Fellowship, a Diane Denson Fellowship, and a Susan G. Komen for the Cure Postdoctoral Fellowship PDF79906 (C. Bartholomeusz).

Abbreviations

PEA-15, phospho-enriched protein in astrocytes
MAPK, mitogen-activated protein kinase
ERK, extracellular signal-regulated kinase
pERK, phosphorylated ERK
FBS, fetal bovine serum
HA, hemagglutinin
GFP, green fluorescence protein
CMV, cytomegalovirus
MOI, multiplicities of infection
Ad, adenovirus
h, hour (s)
min, minute (s)

References

1. Bast RC Jr, Feeney M, Lazarus H, Nadler LM, Colvin RB, Knapp RC. Reactivity of a monoclonal antibody with human ovarian carcinoma. J Clin Invest 1981;68:1331–1337. [PubMed: 7028788]
2. Bartholomeusz C, Itamochi H, Nitta M, Saya H, Ginsberg MH, Ueno NT. Antitumor effect of E1A in ovarian cancer by cytoplasmic sequestration of activated ERK by PEA15. Oncogene 2006;25:79–90. [PubMed: 16170361]
3. Formstecher E, Ramos JW, Fauquet M, et al. PEA-15 mediates cytoplasmic sequestration of ERK MAP kinase. Dev Cell 2001;1:239–250. [PubMed: 11702783]
4. Shinojima N, Yokoyama T, Kondo Y, Kondo S. Roles of the Akt/mTOR/p70S6K and ERK1/2 signaling pathways in curcumin-induced autophagy. Autophagy 2007;3:635–637. [PubMed: 17786026]
5. Ogier-Denis E, Pattingre S, El Benna J, Codogno P. Erk1/2-dependent phosphorylation of Galpha-interacting protein stimulates its GTPase accelerating activity and autophagy in human colon cancer cells. The Journal of biological chemistry 2000;275:39090–39095. [PubMed: 10993892]
6. Pattingre S, Bauvy C, Codogno P. Amino acids interfere with the ERK1/2-dependent control of macroautophagy by controlling the activation of Raf-1 in human colon cancer HT-29 cells. The Journal of biological chemistry 2003;278:16667–16674. [PubMed: 12609989]
7. Aoki H, Takada Y, Kondo S, Sawaya R, Aggarwal B, Kondo Y. Evidence That Curcumin Suppresses the Growth of Malignant Gliomas In Vitro and In Vivo Through Induction of Autophagy: Role of Akt and ERK Signaling Pathways. Molecular pharmacology 2007;72:29–39. [PubMed: 17395690]
8. Corcelle E, Nebout M, Bekri S, et al. Disruption of autophagy at the maturation step by `the carcinogen lindane is associated with the sustained mitogen-activated protein kinase/extracellular signal-regulated kinase activity. Cancer research 2006;66:6861–6870. [PubMed: 16818664]
9. He TC, Zhou S, da Costa LT, Yu J, Kinzler KW, Vogelstein B. A simplified system for generating recombinant adenoviruses. Proc Natl Acad Sci U S A 1998;95:2509–2514. [PubMed: 9482916]
10. Ueno NT, Bartholomeusz C, Herrmann JL, et al. E1A-mediated paclitaxel sensitization in HER-2/neu-overexpressing ovarian cancer SKOV3.ip1 through apoptosis involving the caspase-3 pathway. Clin Cancer Res 2000;6:250–259. [PubMed: 10656456]
11. Hao C, Beguinot F, Condorelli G, et al. Induction and intracellular regulation of tumor necrosis factor-related apoptosis-inducing ligand (TRAIL) mediated apotosis in human malignant glioma cells. Cancer research 2001;61:1162–1170. [PubMed: 11221847]
12. Zhang Y, Yu D, Xia W, Hung MC. HER-2/neu-targeting cancer therapy via adenovirus-mediated E1A delivery in an animal model. Oncogene 1995;10:1947–1954. [PubMed: 7761095]
13. Rosen DG, Yang G, Cai KQ, et al. Subcellular localization of p27kip1 expression predicts poor prognosis in human ovarian cancer. Clin Cancer Res 2005;11:632–637. [PubMed: 15701850]
14. Rosen DG, Mercado-Uribe I, Yang G, et al. The role of constitutively active signal transducer and activator of transcription 3 in ovarian tumorigenesis and prognosis. Cancer 2006;107:2730–2740. [PubMed: 17063503]

15. Rosen DG, Yang G, Deavers MT, et al. Cyclin E expression is correlated with tumor progression and predicts a poor prognosis in patients with ovarian carcinoma. Cancer 2006;106:1925–1932. [PubMed: 16568440]

16. Wang H, Rosen DG, Fuller GN, Zhang W, Liu J. Insulin-like growth factor-binding protein 2 and 5 are differentially regulated in ovarian cancer of different histologic types. Mod Pathol 2006;19:1149–1156. [PubMed: 16729015]

17. Marx D, Binder C, Meden H, et al. Differential expression of apoptosis associated genes bax and bcl-2 in ovarian cancer. Anticancer Res 1997;17:2233–2240. [PubMed: 9216694]

18. Avvakumov N, Wheeler R, D'Halluin JC, Mymryk JS. Comparative sequence analysis of the largest E1A proteins of human and simian adenoviruses. J Virol 2002;76:7968–7975. [PubMed: 12134001]

19. Daido S, Kanzawa T, Yamamoto A, Takeuchi H, Kondo Y, Kondo S. Pivotal role of the cell death factor BNIP3 in ceramide-induced autophagic cell death in malignant glioma cells. Cancer research 2004;64:4286–4293. [PubMed: 15205343]

20. Ramos JW, Hughes PE, Renshaw MW, et al. Death effector domain protein PEA-15 potentiates Ras activation of extracellular signal receptor-activated kinase by an adhesion- independent mechanism. Molecular biology of the cell 2000;11:2863–2872. [PubMed: 10982386]

21. Levine B, Yuan J. Autophagy in cell death: an innocent convict? J Clin Invest 2005;115:2679–2688. [PubMed: 16200202]

22. Ito H, Aoki H, Kuhnel F, et al. Autophagic cell death of malignant glioma cells induced by a conditionally replicating adenovirus. Journal of the National Cancer Institute 2006;98:625–636. [PubMed: 16670388]

23. Zhu JH, Horbinski C, Guo F, Watkins S, Uchiyama Y, Chu CT. Regulation of autophagy by extracellular signal-regulated protein kinases during 1-methyl-4-phenylpyridinium-induced cell death. The American journal of pathology 2007;170:75–86. [PubMed: 17200184]

24. Simone C. Signal-dependent control of autophagy and cell death in colorectal cancer cell: the role of the p38 pathway. Autophagy 2007;3:468–471. [PubMed: 17495519]

25. Kondo Y, Kanzawa T, Sawaya R, Kondo S. The role of autophagy in cancer development and response to therapy. Nat Rev Cancer 2005;5:726–734. [PubMed: 16148885]

26. Cui Q, Tashiro S, Onodera S, Minami M, Ikejima T. Oridonin induced autophagy in human cervical carcinoma HeLa cells through Ras, JNK, and P38 regulation. Journal of pharmacological sciences 2007;105:317–325. [PubMed: 18094523]

27. Ellington AA, Berhow MA, Singletary KW. Inhibition of Akt signaling and enhanced ERK1/2 activity are involved in induction of macroautophagy by triterpenoid B-group soyasaponins in colon cancer cells. Carcinogenesis 2006;27:298–306. [PubMed: 16113053]

28. Newman RA, Kondo Y, Yokoyama T, et al. Autophagic cell death of human pancreatic tumor cells mediated by oleandrin, a lipid-soluble cardiac glycoside. Integrative cancer therapies 2007;6:354–364. [PubMed: 18048883]

29. Vaidyanathan H, Opoku-Ansah J, Pastorino S, Renganathan H, Matter ML, Ramos JW. ERK MAP kinase is targeted to RSK2 by the phosphoprotein PEA-15. Proceedings of the National Academy of Sciences of the United States of America 2007;104:19837–19842. [PubMed: 18077417]

30. Glading A, Koziol JA, Krueger J, Ginsberg MH. PEA-15 inhibits tumor cell invasion by binding to extracellular signal-regulated kinase 1/2. Cancer research 2007;67:1536–1544. [PubMed: 17308092]

31. Krueger J, Chou FL, Glading A, Schaefer E, Ginsberg MH. Phosphorylation of Phosphoprotein Enriched in Astrocytes (PEA15) Regulates ERK-dependent Transcription and Cell Proliferation. Molecular biology of the cell 2005;16:3552–3561. [PubMed: 15917297]

32. Renganathan H, Vaidyanathan H, Knapinska A, Ramos JW. Phosphorylation of PEA-15 Switches its Binding Specificity from ERK MAP kinase to FADD. BiochemJ 2005;390:729–735. [PubMed: 15916534]

33. Renault-Mihara F, Beuvon F, Iturrioz X, et al. Phosphoprotein Enriched in Astrocytes-15 kDa Expression Inhibits Astrocyte Migration by a Protein Kinase C{delta}-dependent Mechanism. Molecular biology of the cell 2006;17:5141–5152. [PubMed: 16987961]

34. Gaumont-Leclerc MF, Mukhopadhyay UK, Goumard S, Ferbeyre G. PEA-15 is inhibited by adenovirus E1A and plays a role in ERK nuclear export and Ras-induced senescence. The Journal of biological chemistry 2004;279:46802–46809. [PubMed: 15331596]

35. Condorelli G, Vigliotta G, Cafieri A, et al. PED/PEA-15: an anti-apoptotic molecule that regulates FAS/TNFR1-induced apoptosis. Oncogene 1999;18:4409–4415. [PubMed: 10442631]

36. Kitsberg D, Formstecher E, Fauquet M, et al. Knock-out of the neural death effector domain protein PEA-15 demonstrates that its expression protects astrocytes from TNFalpha- induced apoptosis. J Neurosci 1999;19:8244–8251. [PubMed: 10493725]

37. Trencia A, Perfetti A, Cassese A, et al. Protein kinase B/Akt binds and phosphorylates PED/PEA-15, stabilizing its antiapoptotic action. Mol Cell Biol 2003;23:4511–4521. [PubMed: 12808093]

38. Formisano P, Perruolo G, Libertini S, et al. Raised expression of the antiapoptotic protein ped/pea-15 increases susceptibility to chemically induced skin tumor development. Oncogene 2005;24:7012–7021. [PubMed: 16044159]

39. Dong G, Loukinova E, Chen Z, et al. Molecular profiling of transformed and metastatic murine squamous carcinoma cells by differential display and cDNA microarray reveals altered expression of multiple genes related to growth, apoptosis, angiogenesis, and the NF-kappaB signal pathway. Cancer research 2001;61:4797–4808. [PubMed: 11406555]

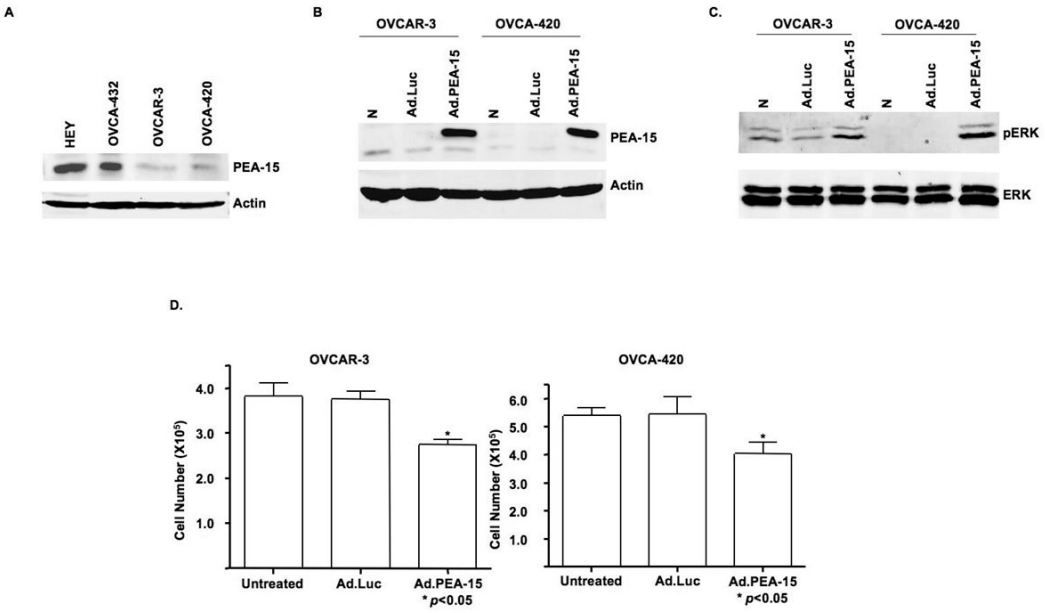

Figure 1. Ad.PEA-15 inhibits cell growth and increases the expression of pERK in ovarian cancer cells

A, Western blot analysis showed heterogenous PEA-15 protein expression in four ovarian cancer cell lines. Equal loading was confirmed by blotting with an anti-actin antibody. Low PEA-15 expression was seen in OVCAR-3 and OVCA420 cells and high expression was seen in OVCA-432 and HEY cells. *B*, Western blotting verified overexpression of PEA-15 in OVCAR-3 and OVCA-420 cells 48 h after transfection with Ad.PEA-15. *C*, PEA-15 overexpression produced by transfection with Ad.PEA-15 induced pERK expression in OVCAR-3 and OVCA-420 cells. *D*, OVCAR-3 and OVCA-420 cells were untreated or infected with Ad.Luc or Ad.PEA-15 for 3 days, after which cells were stained with trypan blue and counted. PEA-15 had significant cytotoxicity ($P < 0.05$).

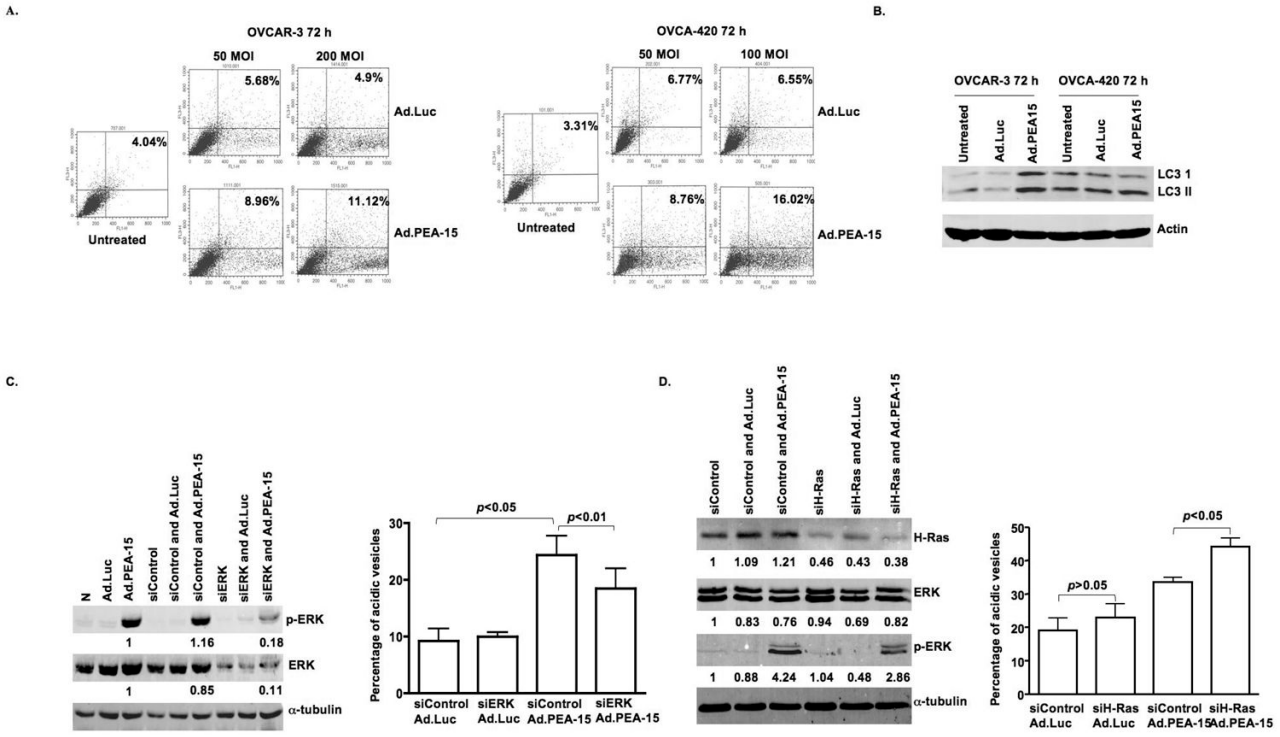

Figure 2. Ad.PEA-15 induces autophagy in ovarian cancer cells in a dose-dependent manner

A, Ad.PEA-15 increased the percentage of cells with vesicular organelles. OVCAR-3 and OVCA-420 cells were untreated or infected with Ad.Luc or Ad.PEA-15 at the indicated multiplicities of infection for 72 h. Cells were stained with acridine orange and analyzed by flow cytometry, and the percentage of cells with acidic vesicular organelles was recorded (FL1-H, green fluorescence intensity; FL3-H, red fluorescence). *B*, Ad.PEA-15 increased LC3 I and LC3 II. OVCAR-3 and OVCA-420 cells were untreated or infected with Ad.Luc or Ad.PEA-15 at a multiplicity of infection of 200 or 100 for 72 h. *C*, siRNA against ERK suppressed both pERK and ERK expression. OVCA-420 cells were transfected with siERK for 48 h, infected with Ad.PEA-15 for 72 h, and then subjected to western blot analysis for pERK1/2, ERK, and α-tubulin, OVCA-420 cells were treated with siERK for 48 h, infected with Ad.PEA-15 for 72 h, and subjected to acridine orange staining. siRNA against ERK decreased the percentage of cells with vesicular organelles. *D*, siRNA against H-Ras increased the percentage of cells with vesicular organelles. OVCA-420 cells were treated with siH-Ras for 48 h, infected with Ad.PEA-15 for 72 h, and subjected to western blot analysis and acridine orange staining recorded (FL1-H, green fluorescence intensity; FL3-H, red fluorescence).

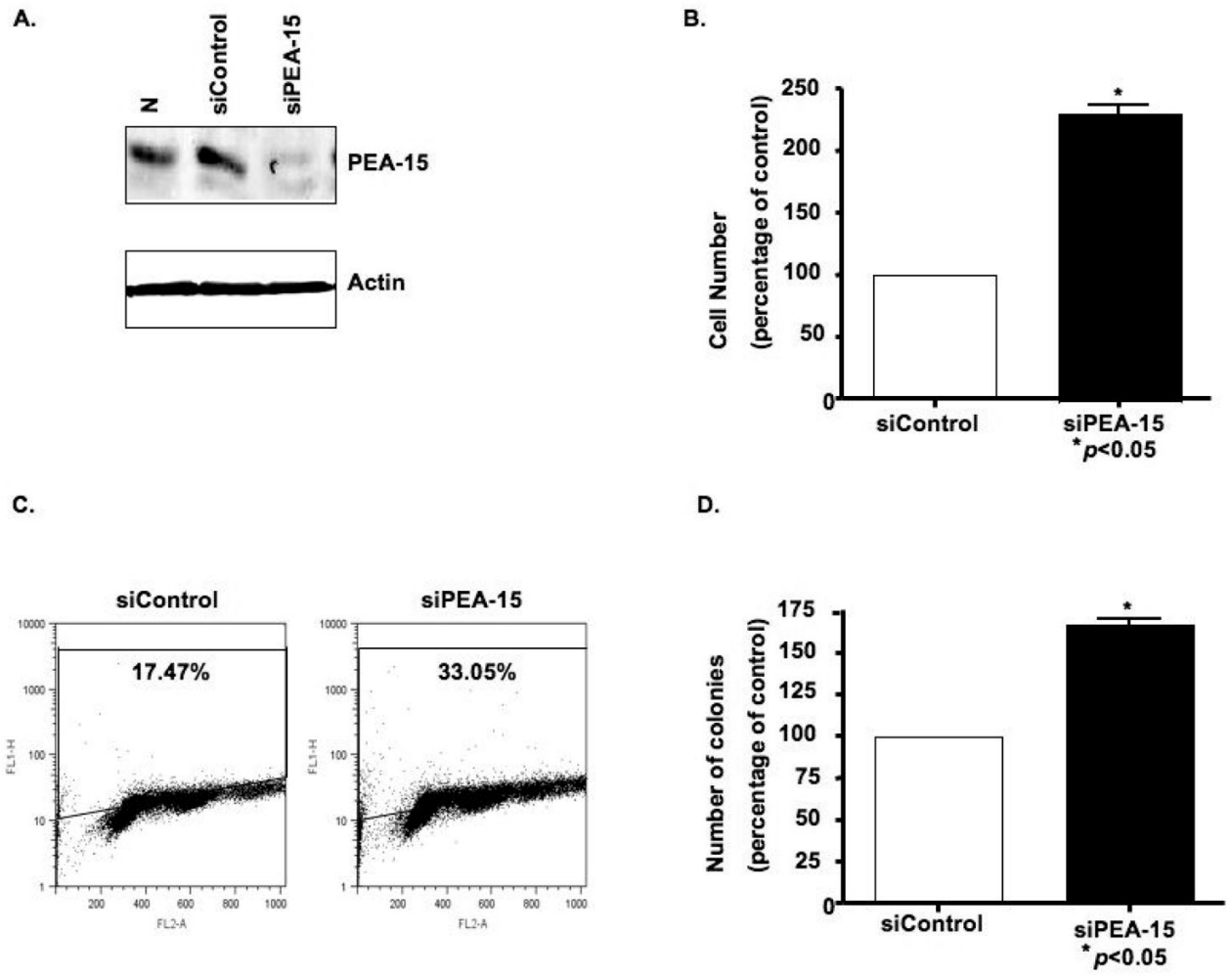

Figure 3. Depletion of PEA-15 leads to increased proliferation and colony formation in high-PEA-15-expressing OVCA-432 cells

A, A 21-nt siRNA sequence targeting PEA-15 reduced the expression of PEA-15 in OVCA-432 cells at 72 h after transfection, as demonstrated by western blot analysis. *B and C*, OVCA-432 cells were transfected with siRNA control or siRNA against PEA-15 for 48 h, after which proliferation was assessed by counting cells after trypan blue staining (*B*) or by incubating cells with bromodeoxyuridine for 30 min, staining them with anti-bromodeoxyuridine-fluorescein isothyocyanate for 30 min, and then sorting them by flow cytometry (*C*). The vertical axis (log scale) shows bromodeoxyuridine incorporation; the horizontal axis (linear scale) shows total DNA. *D*, Soft agar colony formation was assessed by transfecting OVCA-432 cells with siRNA control or siRNA-PEA-15 for 48 h, after which cells were plated, incubated for 3 weeks, and stained with *p*-iodonitrotetrazolium violet and colonies were counted. The results shown here are representative of two independent assays, each done in triplicate.

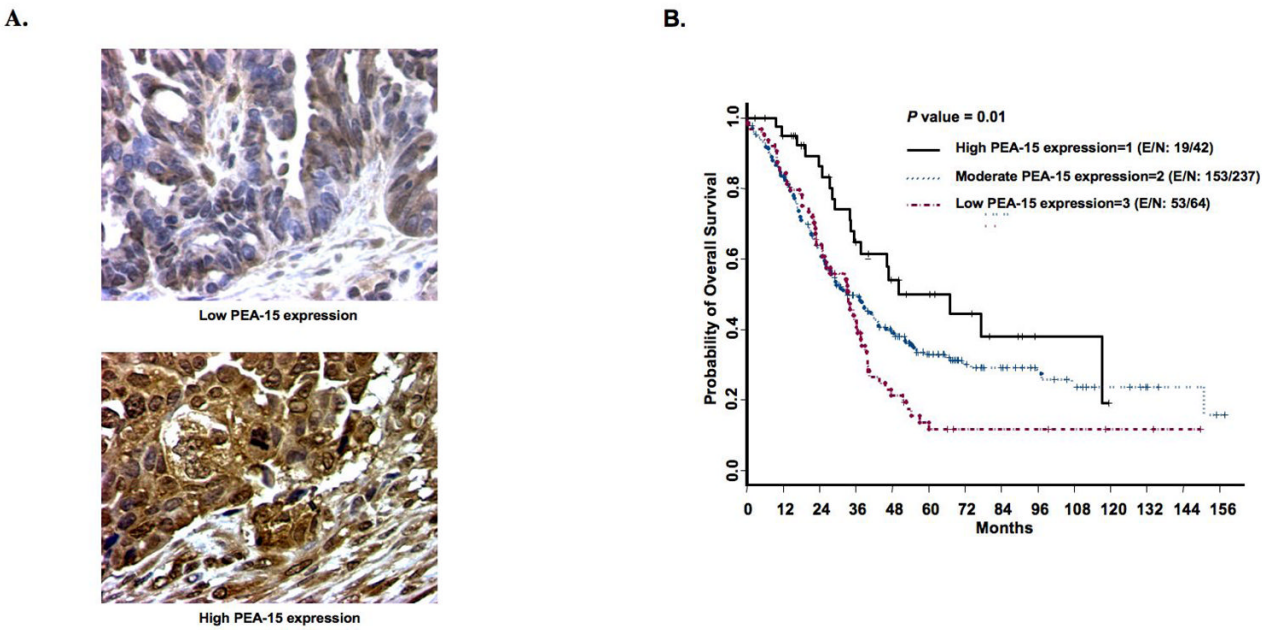

Figure 4. PEA-15 expression and survival in women with ovarian cancer

A, PEA-15 expression on representative sections of ovarian histospots on a tumor microarray. Tumors showed predominantly cytoplasmic staining with some perinuclear and nuclear staining. *B*, Kaplan-Meier curve showing overall survival. PEA-15 expression was associated with significantly improved overall survival ($P = 0.01$) in women with ovarian cancer [E/N = events/ total observations].

Table 1

Patient characteristics

Characteristic	Number of patients (%)	
Histopathologic diagnosis		
Clear cell carcinoma	12	(3.5)
Endometrioid adenocarcinoma	30	(8.7)
Malignant mixed Mullerian tumor	10	(2.9)
Mucinous adenocarcinoma	7	(2.0)
Poorly differentiated carcinoma	14	(4.1)
Serous adenocarcinoma	264	(77.0)
Transitional cell carcinoma	6	(1.7)
Disease stage		
I	13	(3.8)
II	22	(6.4)
III	232	(67.6)
IV	62	(18.1)
Unknown	14	(4.1)
Nuclear grade		
1	15	(4.4)
2	15	(4.4)
3	312	(91.0)
Unknown	1	(0.3)
Extent of cytoreduction		
Optimal	159	(46.4)
Suboptimal	132	(38.5)
Other	39	(11.4)
Unknown	13	(3.8)
PEA-15 expression		
1 (high)	42	(12.2)
2 (moderate)	237	(69.1)
3 (low)	64	(18.7)

Cancer Res. Author manuscript; available in PMC 2009 November 15.

Table 2

a. Univariable Cox proportional hazards models for overall survival

Prognostic factor comparison	N	Parameter estimate	Standard error	*P* value	Hazard ratio
Age					
Continuous	342	0.016	0.006	0.009	1.016
> 61 years *vs.* ≤ 61 years	342	0.28	0.134	0.036	1.324
Race					
Caucasian *vs.* non-Caucasian	340	0.086	0.158	0.586	1.09
Histopathologic diagnosis	343				
Endometrioid adenocarcinoma					
vs. clear cell carcinoma		−1.361	0.477	0.004	0.256
Others *vs.* clear cell carcinoma		−0.165	0.361	0.648	0.848
Serous adenocarcinoma *vs.*					
Clear cell carcinoma		−0.287	0.416	0.49	0.751
Disease stage	329				
Stage 2 *vs.* stage 1		−0.027	0.628	0.965	0.973
Stage 3 *vs.* stage 1		1.292	0.51	0.011	3.641
Stage 4 *vs.* stage 1		1.686	0.526	0.001	5.397
Stage 4+3 *vs.* stage 1+2		1.371	0.312	< 0.0001	3.941
Stage 3 *vs.* stage 1+2		1.303	0.314	< 0.0001	3.679
Stage 4 *vs.* stage 1+2		1.693	0.339	< 0.0001	5.436
Nuclear grade	342				
3 *vs.* 1+2		1.221	0.326	< 0.0001	3.389
Extent of cytoreduction	291				
Optimal *vs.* suboptimal		−0.834	0.147	< 0.0001	0.434
PEA-15 expression	343				
2 *vs.* 1		0.477	0.243	0.05	1.612
3 *vs.* 1		0.784	0.268	0.003	2.191
3 *vs.* 1+2		0.373	0.158	0.018	1.452

b. Multivariable Cox proportional hazards model for overall survival (n=278).

Variable	Parameter estimate	Standard error	*P* value	Hazard ratio
Age	0.0183	0.007	0.0065	1.018
PEA-15 expression				
2 *vs.* 1	0.508	0.262	0.0527	1.662
3 *vs.* 1	0.680	0.284	0.0167	1.973
Disease stage				
III *vs.* I+II	1.067	0.326	0.0011	2.907
IV *vs.* I+II	1.332	0.352	0.0002	3.789
Extent of cytoreduction				
Optimal *vs.* Suboptimal	−0.6113	0.149	<0.0001	0.543